Supporting Information

Influence of Polymorphism on the Electrochemical Behavior of Dilithium (2,3-Dilithium-oxy)-Terephthalate *vs*. Li

Lou Bernard[1,2], Alia Jouhara[1], Eric Quarez[1], Yanis Levieux-Souid[3], Sophie Le Caër[3], Pierre Tran-Van[2], Stéven Renault[1] and Philippe Poizot[1,*]

1. Nantes Université, CNRS, Institut des Matériaux de Nantes Jean Rouxel, IMN, F-44000 Nantes, France
2. Technocentre Renault, 1 avenue du Golf 78280 Guyancourt, France
3. NIMBE, UMR 3685 CEA, CNRS, Université Paris-Saclay, CEA Saclay, 91191 Gif-sur-Yvette Cedex, France

* Corresponding author: philippe.poizot@cnrs-imn.fr

Table of Content

1. Complementary analytical data of dilithium (3-hydroxy-2-lithium-oxy)terephthalate (Li_2)(Li,H)-*o*-DHT

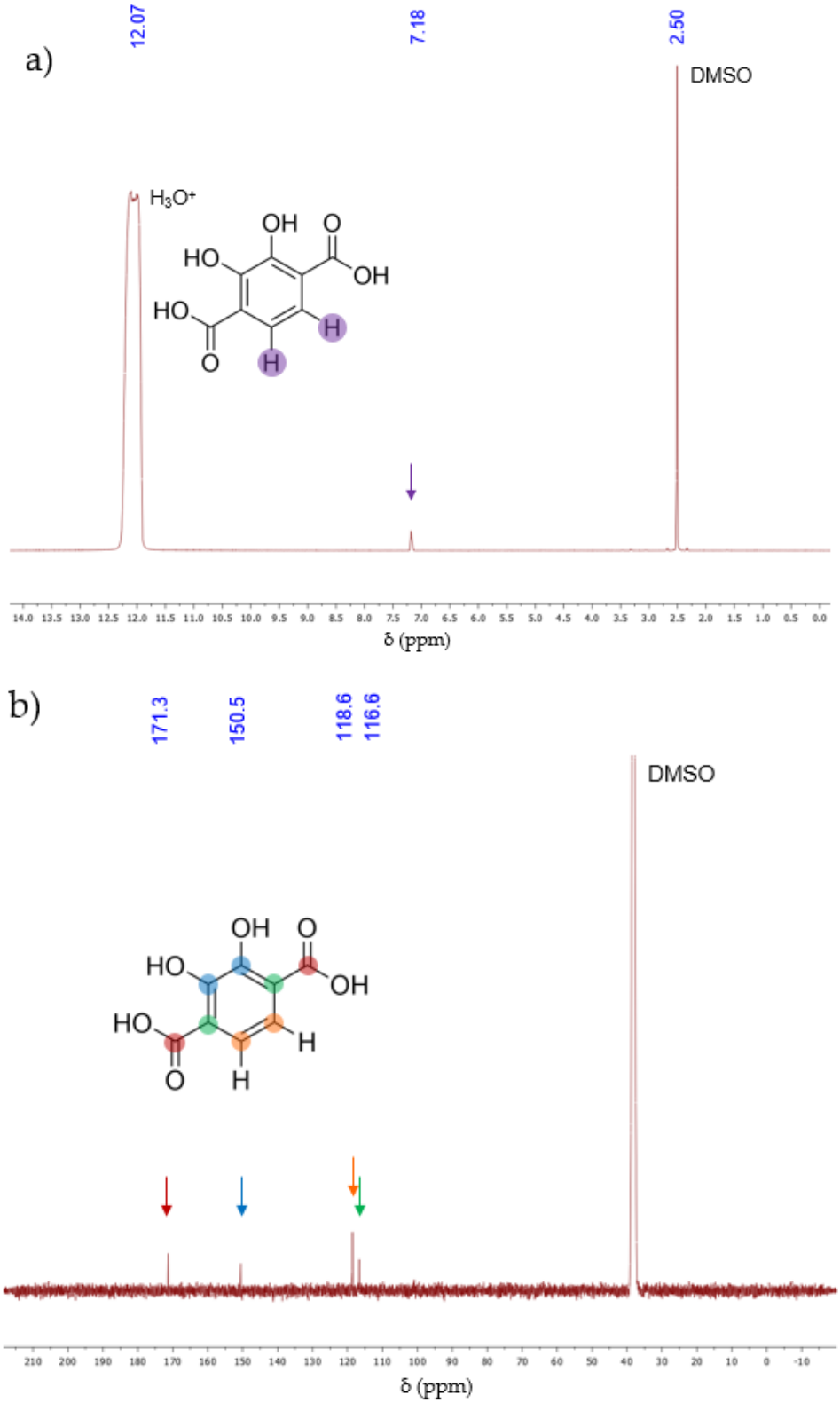

Figure S1. Typical ^{1}H NMR (**a**) and ^{13}C NMR (**b**) spectra of (Li_2)(Li,H)-*o*-DHT measured in H_2SO_4/DMSO-d_6 solution (derivatization reaction).

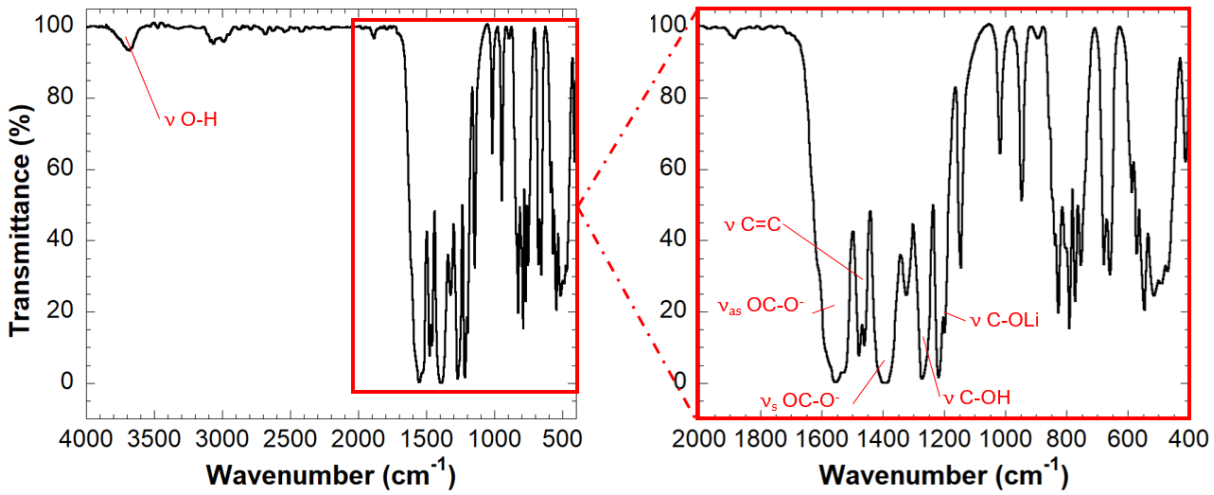

Figure S2. Typical FT-IR spectrum of $(Li_2)(Li,H)$-*o*-DHT (KBr pellet).

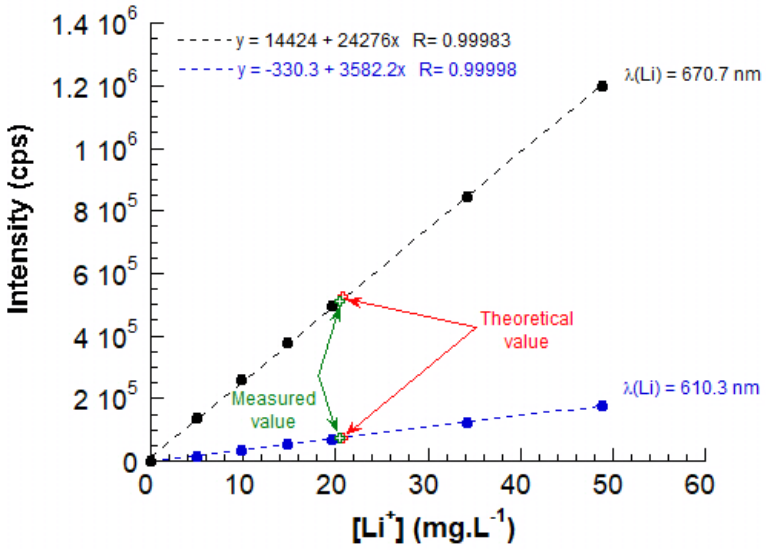

The experimental concentrations found are 20.55 ppm at 610.3 nm and 20.18 ppm at 670.7 nm corresponding to 9.52% ± 0.09 and 9.34% ± 0.48 of atomic lithium, respectively, with an uncertainty of 2σ. These values are in good agreement with the expected theoretical value of 9.64%.

Atom	Theoretical atomic content	Measured atomic content
C	44.50 %	(43.43 ± 1.00)%
H	1.40 %	(1.74 ± 0.02)%
O (deduced)	*44.46 %*	*45.48 %*

Figure S3. Rectilinear calibration graphs for the lithium quantification in $(Li_2)(Li,H)$-*o*-DHT measured by ICP-AES considering two atomic emission lines for Li (610.3 nm and 670.7 nm, respectively). The table summarizes the elemental analysis of both C and H elements obtained by using a combustion analyzer.

a)

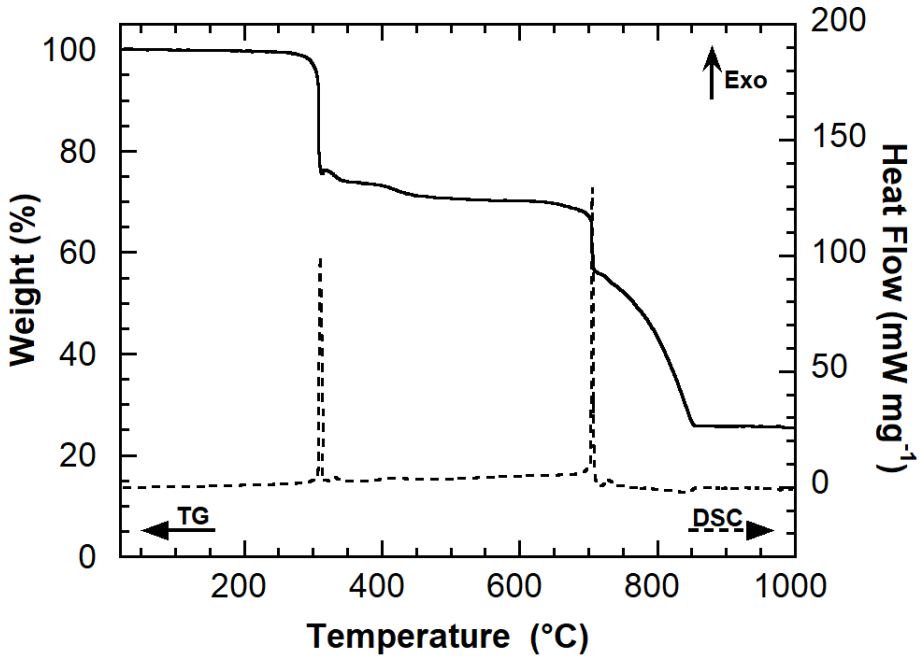

Expected combustion reaction: $2\ C_8H_3Li_3O_{6(s)} + 13\ O_{2(g)} \rightarrow 16\ CO_{2(g)} + 3\ H_2O_{(g)} + 3\ Li_2O_{(s)}$

Theoretical residual mass (Li_2O): ***21 wt%***

b)

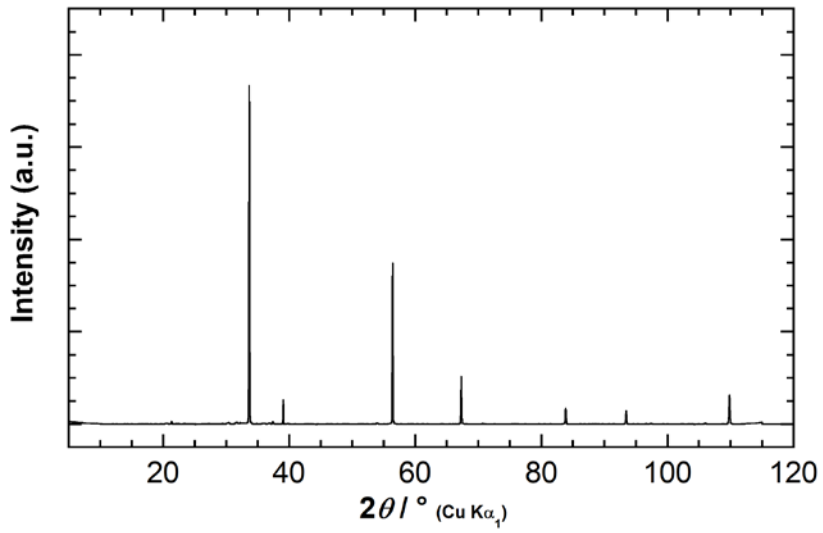

Figure S4. (**a**) Thermal analyses (TG-DSC) of $(Li_2)(Li,H)$-*o*-DHT performed under pure O_2 at a heating rate of 5°C.min^{-1}. (**b**) PXRD pattern of the residue recovered after thermal annealing of $(Li_2)(Li,H)$-*o*-DHT at 1000°C under pure O_2 (combustion) and measured in a quartz capillary due to the small amount of recovered powder. The Bragg peaks correspond to the Li_2O phase (PDF 12-0254), as expected.

2. Complementary analytical data of dilithium (2,3-dilithium-oxy)terephthalate ($(Li_2)(Li_2)$-*o*-DHT or Li_4-*o*-DHT, β-phase)

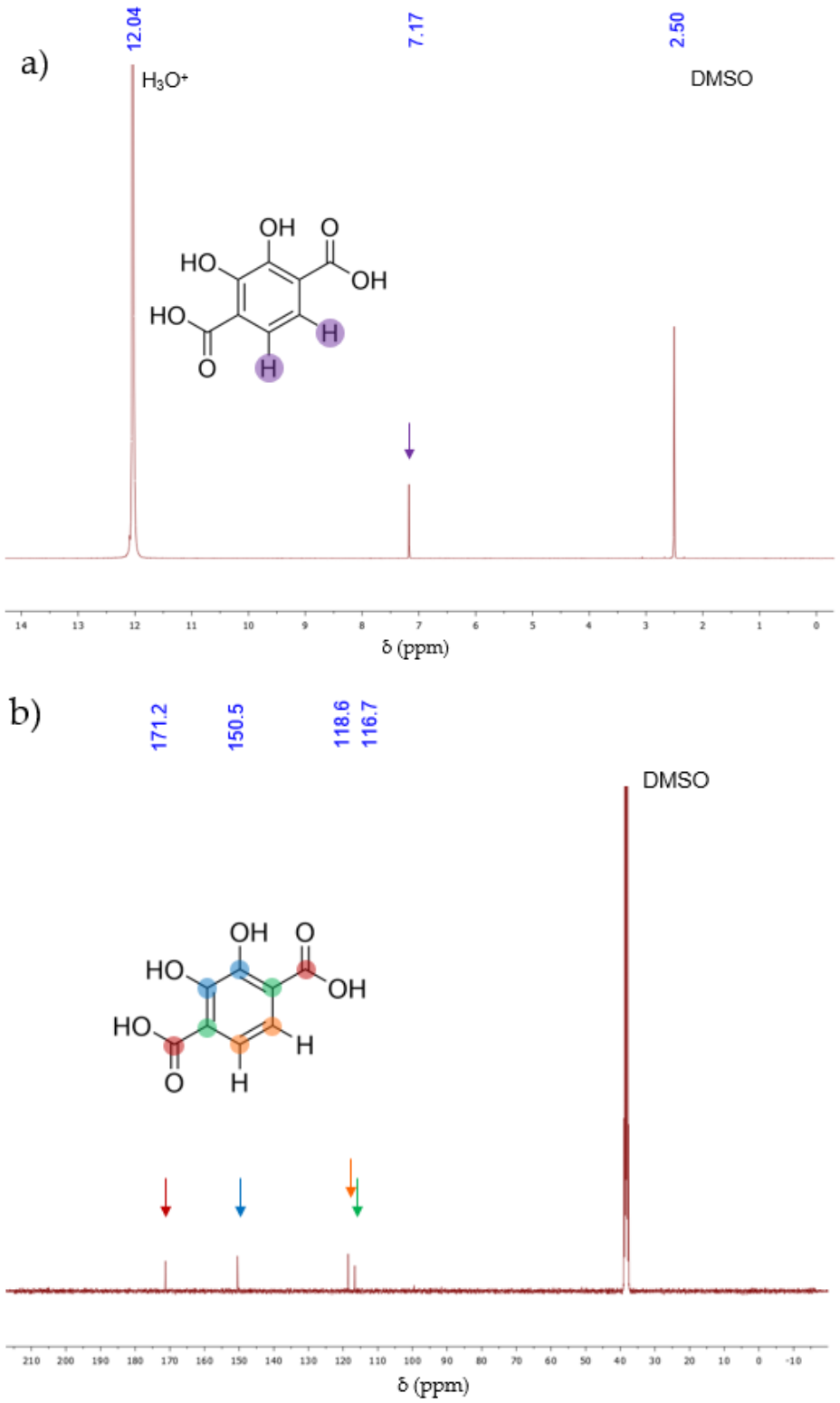

Figure S5. Typical ^{1}H NMR (a) and ^{13}C NMR (b) spectra measured in H_2SO_4/DMSO-d_6 solution (derivatization reaction) of the recovered powder (new phase) after thermal treatment of $(Li_2)(Li,H)$-*o*-DHT at 290 °C during 20 h.

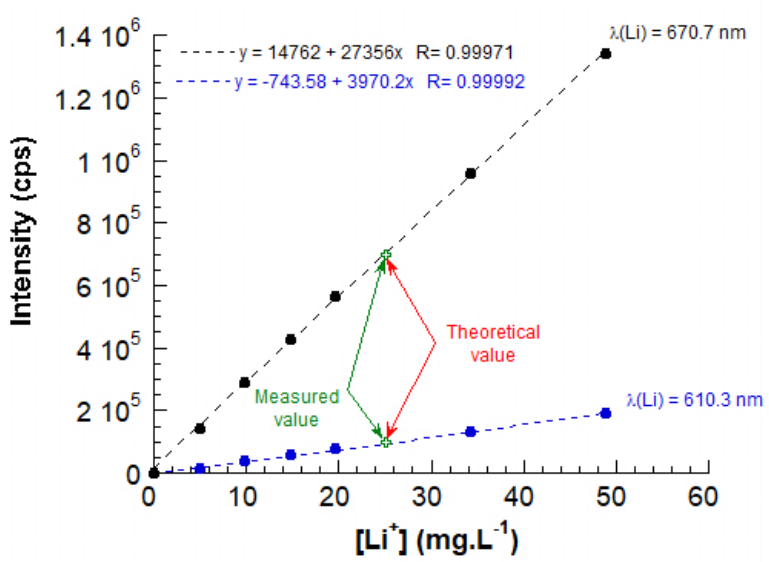

The experimental concentrations found are 25.07 ppm at 610.3 nm and 25.01 ppm at 670.7 nm corresponding to 12.10% ± 0.35 and 12.07% ± 0.57 lithium, respectively, with an uncertainty of 2σ. These values are in good agreement with the expected theoretical value of 12.51%.

Atom	Theoretical atomic content	Measured atomic content
C	43.31 %	(42.69 ± 1.00)%
H	0.91 %	(1.37 ± 0.02)%
O (deduced)	*43.27 %*	*43.72 %*

Figure S6. Rectilinear calibration graphs for the lithium quantification of the recovered powder after thermal treatment of (Li_2)(Li,H)-*o*-DHT at 290°C during 20 h by ICP-AES considering two atomic emission lines for Li (610.3 nm and 670.7 nm, respectively). The table summarizes the elemental analysis of both C and H elements obtained by using a UNICUBE analyzer. The as-obtained phase is ascribed to Li_4-*o*-DHT (β-phase).

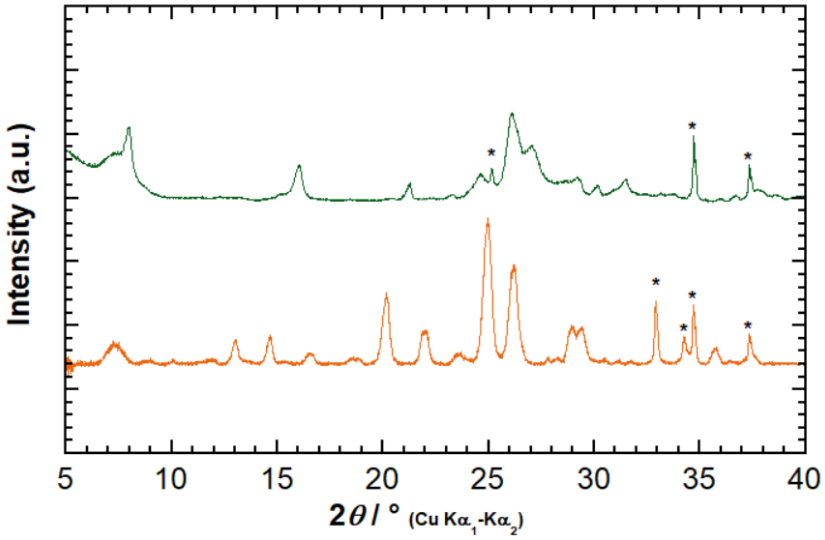

Figure S7. Overlaid of the representative PXRD patterns for Li_4-*o*-DHT (α-phase) in green and Li_4-*o*-DHT (β-phase) in orange extracted from TRXRPD measurements at 245°C [1] and 290°C (Figure 3 in the main text), respectively (* corresponds to the sample holder).

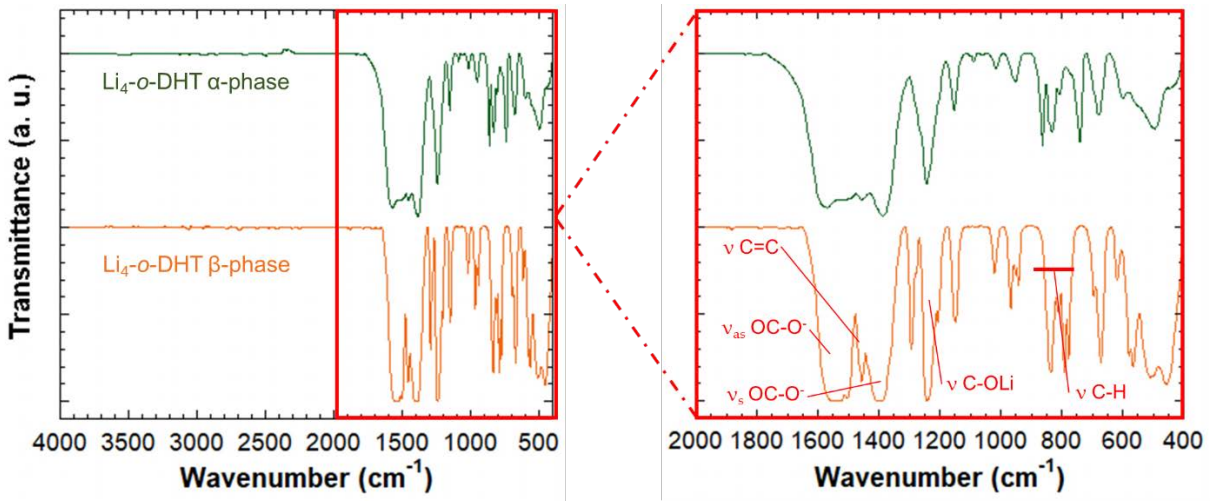

Figure S8. Typical FT-IR spectrum (KBr pellet) of the recovered powder (new phase) after thermal treatment of (Li_2)(Li,H)-*o*-DHT at 290°C during 20 h (in orange); the as-obtained phase is ascribed to Li_4-*o*-DHT (β-phase). The typical FT-IR spectrum (in green) of the previously reported Li_4-*o*-DHT (α-phase) [1] is shown for the sake of comparison. Compared to the FT-IR spectrum of (Li_2)(Li,H)-*o*-DHT (Figure S2), it is noticed the disappearance of (C−OH) vibration band together with the shift of the (C−OLi) vibration band to match the ν(C−OLi) wavenumber of Li_4-*o*-DHT (α-phase).

3. Complementary GC-MS experiments

In order to unravel the role played by the heating rate, the $(Li_2)(Li,H)$-*o*-DHT sample was heated to 300°C at a much higher heating rate than that described in the main text, i.e. at 60°C.min^{-1} instead of 3.5°C.min^{-1}. In this former case, the CO_2 release was measured as 17.7 $\pm$ 1.8 wt%, instead of 10.9 $\pm$ 1.0 wt% for the slowest heating rate. This higher carbon dioxide release is due to secondary thermal reactions which are favored under these conditions. In order to check the nature of the various degradations products that can be formed under such conditions, Gas Chromatography coupled to Mass Spectrometry (GC-MS) experiments were performed. For this, a Gas Chromatograph Agilent 6890 coupled with a mass spectrometer Agilent 5973 MS was used. The mass spectrometer is equipped with an electron impact (EI) source, and a quadrupole mass analyzer. The mass range was 4–160. Helium was used as the vector gas with a flow rate of 2 mL.min^{-1}. Separation was carried out by two distinct separation modes: on one hand, with a CP-PorabondQ (25 m, Ø 0.32 mm) column (Varian), and on the other hand, with a two columns system connected in parallel, a molecular sieve Rt-MSieve 5 Å PLOT (30 m, Ø 0.53 mm) column (Restek) and a Rt-Q-Plot (30 m, ø 0.32 mm) column (Restek). Injector was set at 110°C in splitless mode. Notably, these columns do not allow us to detect catechol, if it is produced.

The chromatogram measured under these conditions is given in Figure S9. With a high heating rate (60°C.min^{-1}), CO_2 is not the only carbonaceous species detected. Other molecules such as methanol, acetone, dimethyl ether and diethyl ether are formed, showing that secondary thermal reactions are favored in this case.

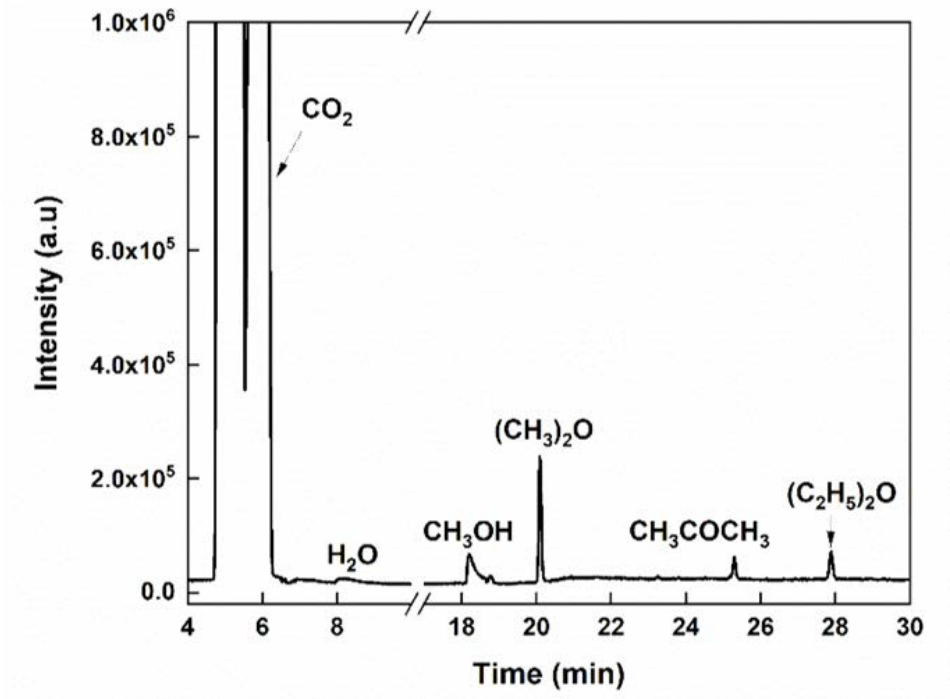

Figure S9. Chromatogram measured after heating of $(Li_2)(Li,H)$-*o*-DHT to 300°C at a heating rate of 60°C.min^{-1}. The presence of acetone may also be due to residues of the cleaning procedure of the ampoules.

4. Complementary data concerning the electrochemical study of Li_4-*o*-DHT (β-phase) vs. Li

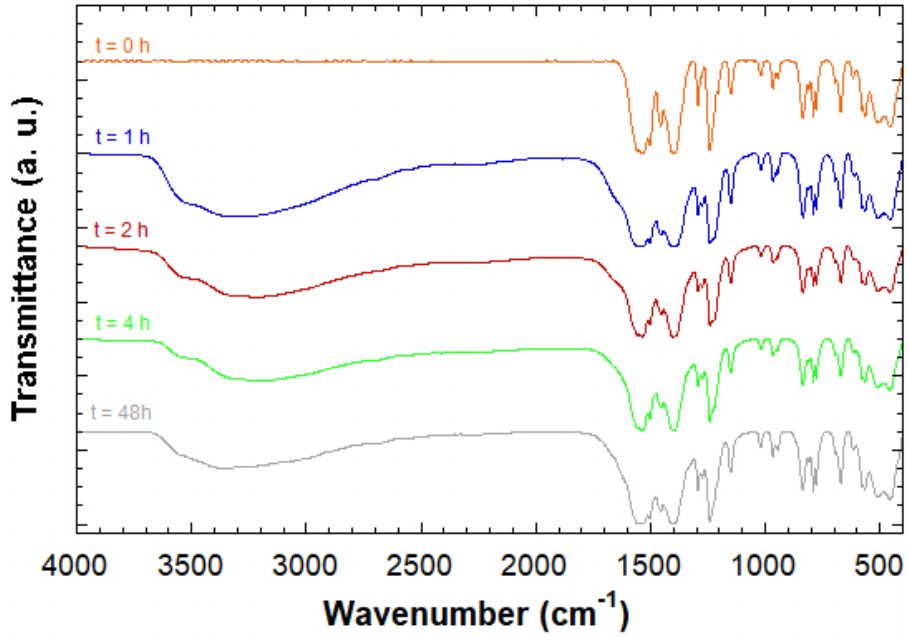

Figure S10. Evolution of FT-IR spectra of Li_4-*o*-DHT (β-phase) after air exposure.

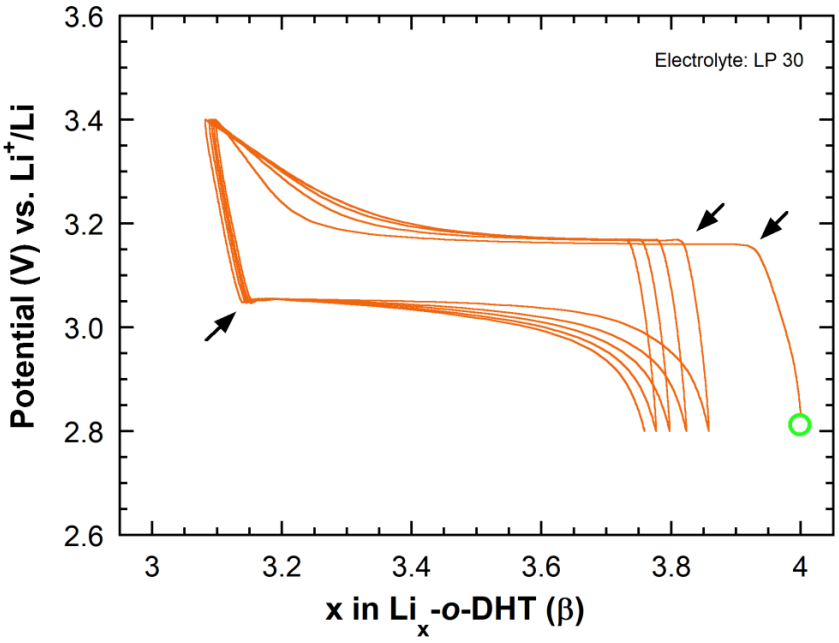

Figure S11. First five cycles of a Li half-cell using Li_4-*o*-DHT (β-phase) as the positive electrode material (carbon additive: 33 wt% KB600) galvanostatically cycled at 1 Li^+/10 h as reported in Figure 6a in the main text by using this time the common "LP30" battery grade electrolyte (i.e., $LiPF_6$ 1 M in EC:DMC 1:1 vol./vol.). Note the reversible capacity measured at the first cycle is a bit lower compared to data reported in Figure 6a in the main text. Arrows highlight again the overpotential activation peaks at the beginning of each two-phase transition.

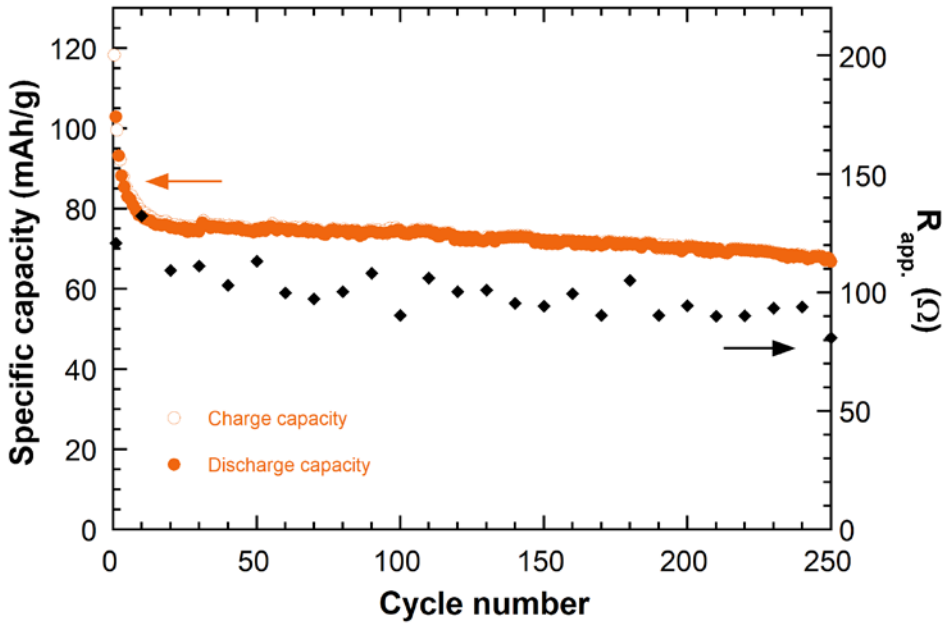

Figure S12. Capacity retention curve upon cycling (from Figure 6b in the main text) together with the corresponding evolution of the apparent cell resistance measured in charge and reported every ten cycles. [Electrolyte: 1 M $LiClO_4$/PC]

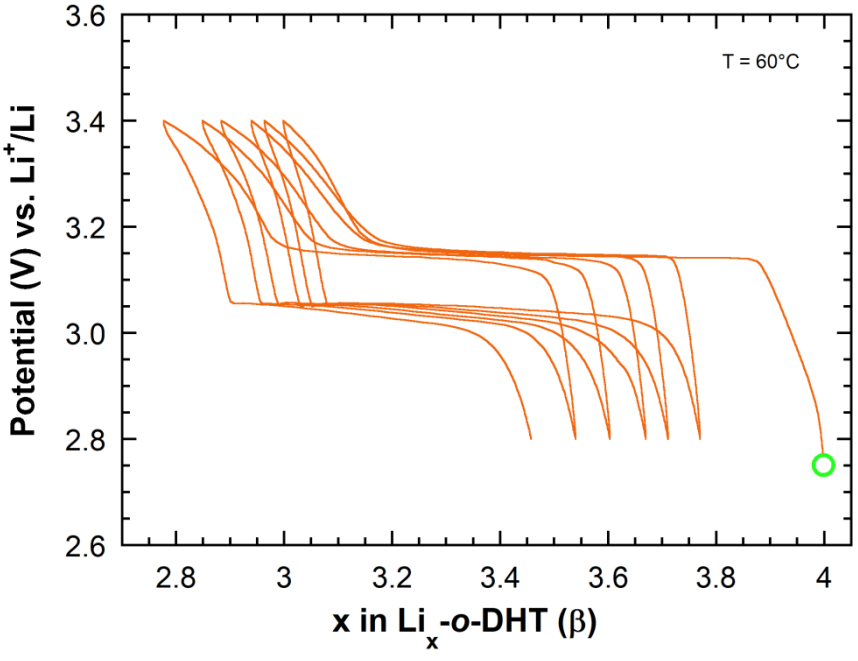

Figure S13. First six cycles of a Li half-cell using Li_4-*o*-DHT (β-phase) as the positive electrode material (carbon additive: 33 wt% KB600) galvanostatically cycled at 1 Li^+/10 h at 60°C. [Electrolyte: 1 M $LiClO_4$/PC; the green circle indicates the starting potential]

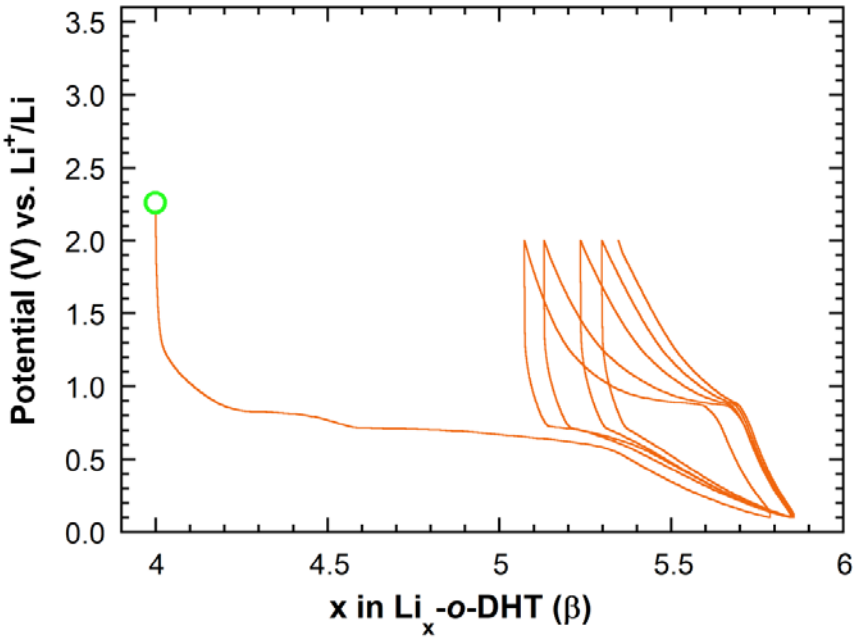

Figure S14. First five cycles of a Li half-cell using Li_4-*o*-DHT (β-phase) as the positive electrode material (carbon additive: 33 wt% C65) galvanostatically cycled at 1 Li^+/10 h (first discharge at 1 Li^+/5 h). [Electrolyte: 1 M $LiClO_4$/PC; the green circle indicates the starting potential]

Reference

1. Gottis, S.; Barrès, A.-L.; Dolhem, F.; Poizot, P. Voltage Gain in Lithiated Enolate-Based Organic Cathode Materials by Isomeric Effect. *ACS Appl. Mater. Interfaces* **2014**, *6*, 10870–10876, doi:10.1021/am405470p.